Article

pubs.acs.org/Biomac

Structure–Function Correlation of Aminated Poly(α)glutamate as siRNA Nanocarriers

Adva Krivitsky,[∥,†] Dina Polyak,[∥,†] Anna Scomparin,[†] Shay Eliyahu,[†] Asaf Ori,[‡] Sharon Avkin-Nachum,[‡] Vadim Krivitsky,[§] and Ronit Satchi-Fainaro*[,†]

[†]Department of Physiology and Pharmacology, Sackler Faculty of Medicine, Room 607, Tel Aviv University, Tel Aviv 69978, Israel

[‡]QBI Enterprise, Ltd., Ness-Ziona 70400, Israel

[§]School of Chemistry, the Raymond and Beverly Sackler Faculty of Exact Sciences, Tel-Aviv University, Tel Aviv 69978, Israel

Supporting Information

ABSTRACT: It has been two decades since cationic polymers were introduced to the world of oligonucleotides delivery. However, the optimal physicochemical properties to make them a successful delivery vehicle are yet unknown. An ideal system became particularly interesting and necessary with the introduction of RNA interference as a promising therapeutic approach. Such nanocarrier should overcome challenges such as low plasma stability, poor cellular internalization and endosomal escape to induce gene silencing. To that end, we synthesized a library of biodegradable aminated poly(α)glutamate varied by amine moieties. In an attempt to elucidate the structure–function relationship, our polyplexes were physicochemically characterized and their silencing activity and cytotoxicity were evaluated. We found several structures that demonstrated improved cellular internalization. These candidates silenced gene expression to less than 50% of their initial levels, while being safe to cells and mice. Based on our research, an improved and promising tailor-designed siRNA delivery platform can be developed.

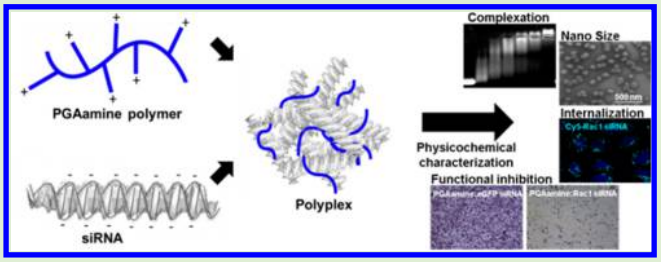

INTRODUCTION

Small interfering RNAs (siRNAs) were first described in the late 20th century as powerful and specific gene regulators.[1−3] Since then, they have been vastly tested for therapeutic applications due to their ability to silence disease-causing genes based on base-pair complementation.[4,5] Various medical uses to siRNA have been suggested; among them are the treatment of viral infections, neurodegenerative disorders and cancer.[6] Due to the siRNA's negative charge, high immunogenicity, and poor serum stability, the use of a delivery vehicle for therapeutic purposes is inevitable.[7,8] Several delivery approaches have been developed, most of them are based on cationic lipids or polymeric carriers that can electrostatically interact with the negatively charged RNA.[9−15] Distinct linear, branched, or globular structures can assemble with siRNA to form liposomal complexes, i.e., lipoplexes,[11] core and shell particles[16] or polymeric complexes, i.e., polyplexes.[9] These nanoparticles can achieve tumor specific targeting by the enhanced permeability and retention (EPR) effect.[17,18] Despite high expectations, siRNA's gene silencing-based therapeutic delivery approaches have encountered pharmacokinetic limitations, such as low stability in solution and aggregation tendency,[7,19−21] short *in vivo* circulation time, fast renal clearance, accumulation in reticuloendothelial system (RES) organs such as liver and lung and toxicity.[7,12,22−28] These limitations have raised the need for proper characterization and the substantial investigation of the relationship between structure, physicochemical properties and activity as a fundamental tool in the quest for the ideal siRNA delivery vehicle. Such attempts were previously performed to investigate the preferred size,[13,14] amine to phosphate ratio (N/P ratio),[13,29,30] the ratio between cationic and hydrophobic content[31] or the size of polyethylene glycol (PEG) used for PEGylation[24] of such delivery systems. In this study, we describe the synthesis and characterization of a poly-α-glutamic acid (PGA) platform to conjugate various amine moieties. PGA is a synthetic biodegradable polymer that is cleaved by cathepsin B, an intracellular cysteine protease that is highly expressed in most tumor tissues.[32] Its upregulation in malignancy results in its secretion to the cell's surface and extracellular matrix.[33] The intracellular, lysosomal, activity of cathepsin B, however, is the one acknowledged as responsible for the *in vivo* cleavage of the PGA polymeric backbone and the release of an active chemotherapeutic drug.[34−36] The enzyme is also largely distributed and active in endosomes, potentially capable of releasing a free and active siRNA from the cleaved-PGA backbone.[37−39] PGA's water-solubility, low immunogenicity and low toxicity at doses required for activity, makes it a great candidate for clinical translation as reflected by the multiple clinical trials performed on paclitaxel polyglumex, a conjugate composed of the chemotherapeutic drug paclitaxel

Received: April 18, 2016
Revised: June 29, 2016
Published: July 5, 2016

DOI: 10.1021/acs.biomac.6b00555
Biomacromolecules 2016, 17, 2787−2800

bound to PGA-based polymer.[40−43] The pendant free γ-carboxyl group in each repeating unit of L-glutamic acid provides functionality for amine-bearing moieties, to which RNA can bind via electrostatic interactions. Poly-aminated PGA is positively charged, thus can internalize to the target cells via electrostatic attraction to the negatively charged cell membrane.[44,45] In addition, multiple amino groups in acidic compartments might behave as proton sponges and lead to rupture of the membranes and a subsequent release of their contents to the cytoplasm, which is the siRNA site of activity.[46,47] We have designed, synthesized, and characterized a library of PGAamine polymers, differing in length and structure of the side-chain amine moiety. Its length ranged between two to six carbons, in the presence or absence of a central secondary amine, bearing a primary or tertiary amine terminus and combinations thereof. We have characterized the physicochemical properties of the various polyplexes formed by our library of PGAamine-based polymers and siRNA, and have shown that the polyplexes varied in their ability to internalize into cells and induce gene silencing. Since amine modifications might alter the biological safety of the PGA backbone, we have evaluated the toxicity of our polymers throughout the manuscript in various *in vitro* and *in vivo* assays. In this study, we aimed to define the requirements for efficient silencing activity resulting from adequate cellular penetration and cellular trafficking.

EXPERIMENTAL SECTION

Materials. All chemicals and solvents were A.R. or HPLC grade. Chemical reagents were purchased from Sigma-Aldrich (Louis, MO, US) and Merck (White House Station, NJ, US). O-benzyl protected glutamic acid (H-Glu(OBzl)-OH) was purchased from Chemimpex (Dillon Drive, IL, US). HPLC grade solvents were from BioLab (Jerusalem, Israel). All tissue culture reagents were purchased from Biological Industries Ltd. (Beit Haemek, Israel), unless otherwise indicated. eGFP siRNA, RAC1 siRNA and Cy5-labeled RAC1 siRNA sequences were obtained from QBI (Rehovot, Israel).

Synthesis of PGAamine Polymers. *Preparation of Poly-α-glutamic Acid.* PGA was synthesized from O-benzyl protected glutamic acid (H-Glu(OBzl)−OH) by n-carboxyanhydride (NCA) polymerization as previously published[48] with the following modifications: A suspension of H-Glu(OBzl)−OH (2.1 g, 8.85 mmol) in dry tetrahydrofuran (THF) (30 mL) was heated to 50 °C. Limonene (1.5 mL, 6.32 mmol) was added prior to the addition of a solution of triphosgene (1.31 g, 8.85 mmol) in dry THF (10 mL). The reaction mixture was stirred under reflux for 3 h at 50 °C under Argon atmosphere. Then, it was bubbled with $Ar_{(g)}$ for an additional 2 h. The resulting solution was precipitated in cold hexane, filtered and recrystallized from a mixture of 5:3 toluene:THF by dropwise addition of cold hexane. The resulting NCA monomer was filtered (1.5 g, 5.7 mmol) and dissolved in dry dichloromethane (DCM) (30 mL). Hexylamine (1.5 μL, 0.0113 mmol) was added, and the reaction left to stir for 7 days at 4 °C. The reaction solution was precipitated in cold ether then kept in −20 °C for 5 h. The resulting poly(γ-benzyl glutamate) was filtered with 0.22 μm filter. Overnight deprotection of the γ-Benzyl was performed in 4 equiv (per carboxylic group) of 48% HBr in trifluoroacetic acid (TFA), the resulting PGA was precipitated in cold ether, and the precipitate was collected by centrifugation at a 50% yield. ^{1}H NMR (D2O; 400 MHz): δ 4.32 (1H, s), 2.36 (2H, s), 2.05, (1H, s), 1.94 (1H, s).

General Preparation of PGAamine Polymers A−I. To a solution of PGA (X mg, X_1 mmol per monomer) in dry dimethylformamide (DMF) (X_2 mL) was added a solution of carbonyldiimidazole (CDI) (Y mg, Y_1 mmol) in dry DMF (Y_2 mL). The reaction mixture was stirred for 1.5 h, at 25 °C, under Argon atmosphere. Tributylamine (Z μL, Z_1 mmol) was added and the reaction left to stir for 5 more min at the same conditions. A solution of the amination reagent (M mmol) in dry DMF (M_1 mL) was added, and the reaction mixture was stirred for an additional 1−2 h at the starting conditions. A solution of a second amination reagent (M_2 mmol) in dry DMF (1 mL) was added, and the reaction mixture was stirred for additional 1−2 h at the starting conditions (relevant only for polyplexes D, E, G and I). A solution of CDI (N mg, N_1 mmol) in dry DMF (N_2 mL) was added, and the reaction mixture was stirred at 25 °C, under Argon for additional 12 h. DMF was removed under reduced pressure and the remaining oily residue was dissolved in water (40 mL) and freeze-dried. Polymers A, B, D, E, G, H, and I underwent acidic deprotection of the Boc group: The resulting solid was dissolved in DCM (5 mL) and TFA (5 mL) was added at 0 °C. The mixture was stirred at 25 °C for 10−20 min then evaporated under reduced pressure. The oily residue was dissolved in double distilled water (DDW) (40 mL), and the aqueous phase was extracted with DCM (2× 50 mL) and diethyl ether (50 mL). The aqueous phase was collected and treated with a 10% NaOH solution to reach pH = 5.5 and then freeze-dried. The remaining solid was dissolved in DDW (20 mL) and dialyzed for 48 h at 4 °C (total of 8 L of DDW). The aqueous phase was collected and freeze-dried to obtain a white powder as a TFA salt. Alternatively, for polymers C and F, DDW (40 mL) was added, and the mixture was treated with 10% HCl solution to pH of 2.5−4.0. The reaction mixture was extracted with chloroform (2× 40 mL) and diethyl ether (50 mL). The aqueous phase was collected and treated with a 10% NaOH solution to pH 5.5−7.0, then freeze-dried. The remaining solid was dissolved in DDW (20 mL) and dialyzed for 48−72 h at 4 °C (total of 6−12 L of DDW). The aqueous phase was collected and freeze-dried to obtain a white powder as a chloride salt.

Table 1 summarizes the synthetic procedures.

Preparation of Polyplexes. All polyplexes were screened for silencing activity at variable terminal nitrogen/phosphate (N/P) ratios (Supplementary Figure 5). For our structure−function evaluation throughout the manuscript, we limited polymer administration to 10 N/P ratio. Polyplexes A, C, D, E, F, and I were prepared at an N/P ratio of 5. Polyplex B was prepared at N/P ratio of 10 due to *in vitro* activity obtained at this ratio. Preparation of polyplexes for all *in vitro* assays and size analysis by DLS: PGAamine polymer was dissolved in nonsupplemented medium from either 1 mg/mL stock solution (for the *in vitro* assays) or 10 mg/mL solution (for the DLS measurements). RNA was added to the polymer's solution at the indicated N/P ratio from a 20 μM solution (for the *in vitro* assays) or from 200 μM solution (for the DLS measurements) and pipetted. All stock solutions were prepared in DDW. Samples were incubated for 20 min then added with 75% (v/v) of full medium (as detailed in the Cell Culture section) before either replacing the cell's medium with the transfection mix or performing a DLS measurement. Phenol-red free DMEM was used for the DLS measurements. Preparation of samples for EMSA: Polymer solution was diluted in DDW from 0.1 mg/mL stock solution in DDW. SiRNA was added from 20 μM stock solution in DDW up to 50 pmol at a final volume of 15 μL and pipetted. Samples were incubated for 20 min before loading on gels. Preparation of samples for Heparin displacement assay: Polymer solution was diluted in DDW from 1 mg/mL stock solution in DDW. SiRNA was added from 20 μM stock solution in DDW up to 50 pmol and pipetted. Samples were incubated for 20 min, then added with 1.5 μL of X10 concentrated phosphate buffered saline (PBS) and pipetted. Preparation of samples for Zeta potential analysis: polymer was diluted in DDW to 0.2 mg/mL solution from 10 mg/mL stock solution in DDW; siRNA was added at the indicated N/P ratio from 200 μM stock (in DDW) and pipetted. Samples were incubated for 20 min then 10% (v/v) of 155 mM PBS were added to give a final solution of 15 mM PBS before performing a zetasizer measurement. Preparation of samples for SEM: 10 μL of polymer solution were diluted in DDW to 0.1 mg/mL solution from 1 mg/mL stock solution in DDW; siRNA was added at the indicated N/P ratio from 20 μM stock (in DDW) and pipetted. Samples were incubated for 20 min. Preparation of samples for *in vivo*: polymer solution from 10 mg/mL stock (in DDW) was diluted in DDW. SiRNA was added at the indicated doses and N/P ratios from 200 μM stock (in DDW) and pipetted. Samples were incubated for 20 min, prior to the addition of 1/10 (% v/v) X10 concentrated PBS.

DOI: 10.1021/acs.biomac.6b00555
Biomacromolecules 2016, 17, 2787−2800

Table 1. Summary of the Synthetic Procedures Used for PGAamine Polymers A–I

polymer	name of the compound	amount of PGA precursor used for the procedure	amount of CDI added (Ist addition)	amount of Tributylamine added	amination reagents, their molarity and volume of solvent they were dissolved in	amount of CDI added (IInd addition)	Boc acidic deprotection	yield	^{1}H NMR (D2O; 400 MHz)
A	*γ-ethylenediamino-L-polyglutamate*	X = 50	Y = 75	Z = 94	Boc- ethylenediamine	N = 133	Yes	41%	δ 4.32 (1H, s), 3.45 (2H, s), 3.27 (2H, s), 2.36 (2H, s), 2.05, (1H, s), 1.94 (1H, s).
		X_1 = 0.38	Y_1 = 0.46	Z_1 = 0.36	M = 0.42	N_1 = 0.82			
		X_2 = 1	Y_2 = 1		M_1= 1.5	N_2 = 1			
B	*γ-hexydiamino-L-polyglutamate*	X = 50	Y = 192	Z = 92	Boc-1, 6-diaminohexane		Yes	31%	δ 4.26 (1H, s), 3.13 (2H, s), 2.93 (2H, s), 2.32 (2H, s), 2.08, (1H, s), 1.97 (1H, s), 1.61 (2H, s), 1.47 (2H, s), 1.32 (4H, s).
		X_1 = 0.38	Y_1 = 1.20	Z_1 = 0.39	M = 1.96				
		X_2 = 1	Y_2 = 1		M_1 = 1				
C	*γ-3-Dimethylamino-1-propylamino-L-polyglutamate*	X = 51	Y = 201	Z = 92	3-(dimethylamine)-1-propylamine		No	45%	δ 4.29 (1H, s), 3.25 (2H, s), 3.01 (2H, s), 2.81 (6H, s), 2.33, (2H, s), 2.05–1.90 (2H, bs), 1.90 (2H, s).
		X_1 = 0.39	Y_1 = 1.24	Z_1 = 0.39	M = 3.98				
		X_2 = 1	Y_2 = 1.5		M_1 = 1				
D	*γ-3-Dimethylamino-1-propylamino-ethylendiamino-L-polyglutamate*	X = 50	Y = 70	Z = 92	3-dimethylamine-1-propylamine	N = 125	Yes	22%	δ 4.20 (1H, s), 4.04 (0.3H, s) 3.37 (2H, s), 3.15 (1H, s), 3.02 (2H, s), 2.76, (3H, s), 2.26 (3H, s), 1.98–1.81 (4H, bs)
		X_1 = 0.38	Y_1 = 0.43	Z_1 = 0.39	M = 3.98	N_1 = 0.477			
		X_2 = 1	Y_2 = 1		M_1 = 1	N_2 = 0.7			
					Boc-ethylenediamineM_2= 0.31				
E	*γ-6-Dimethylamino-hexyl-diaminohex-ane-L-polygluta-mate*	X = 41	Y = 56	Z = 83	6-Dimethylhexyamine M = 0.09 M_1 = 1	N = 103	Yes	32%	δ 4.16 (1H, s), 3.03 (3H, s), 2.86 (1H, s), 2.73 (1H, s), 2.22 (2H, s), 1.98–1.86 (2H, bs), 1.53 (3H, s), 1.98 (3H, s), 1.23 (1H, s).
		X_1=0.32	Y_1 = 0.34	Z_1 = 0.32	Boc-diaminohexaneM_2= 0.26	N_1 = 0.63			
		X_2= 2	Y_2 = 1			N_2 = 1			
F	*γ-Dimethyldipro-pylenetriamine-L-polyglutamate*	X = 40	Y = 60	Z = 73	Dimethyldipropylenetriamine	*N* = 106	No	35%	δ 4.27 (1H, s), 3.19 (3H, s), 2.59 (4H, s), 2.41 (2H, s), 2.33 (2H, s), 2.23 (6H, s), 2.08–1.97 (2H, bs), 1.67 (4H, s)
		X_1=0.31	Y_1 = 0.37	Z_1 = 0.31	M = 0.34	N_1 = 0.65			
		X_2= 1	Y_2 = 1		M_1= 2	N_2 = 2			
G	*γ-Dimethyldipropyle-netriamine-diami-nohexane-L-poly-glutamate*	X = 41	Y = 57	Z = 83	6-dimethyldipropylenetriamine	*N* = 105	Yes	36%	δ 4.32–4.10 (1H, bs), 3.18–1.29 (16H, m).
		X_1=0.32	Y_1 = 0.34	Z_1 = 0.32	M = 0.13 M_1= 1	N_1 = 0.65			
					boc-diaminohexaneM_2= 0.22	N_2 = 1			
		X_2= 1	Y_2 = 1						
H	*γ-2, 2-iminodiethylamino-L-polyglutamate*	X = 47	Y = 67	Z = 87	Boc-2, 2-iminodiethylamine	*N* = 124	Yes	42%	δ 4.23 (1H, s), 3.49 (2H, s), 3.33–3.22 (6H, m), 3.1 (1H, s), 2.27 (2H, s), 2.01–1.91 (2H, bs).
		X_1=0.36	Y_1 = 0.41	Z_1 = 0.36	M = 0.43	N_1 = 0.77			
		X_2= 1	Y_2 = 1		M_1= 1.5	N_2 = 1			
I	*γ-2, 2-iminodiethylamino-dimethydipropyle-netriamino-L-polyglutamate*	X = 40	Y = 67	Z = 74	boc-2, 2-iminodiethylamine	*N* = 100	Yes	30%	δ 4.12 (1H, s), 3.07–3.74 (15H, m).
		X_1=0.31	Y_1 = 0.41	Z_1 = 0.31	M = 0.1	N_1 = 0.62			
		X_2= 1	Y_2 = 1		M_1= 1	N_2 = 1			
					Dimethydipropylenetriamine M_2= 0.24				

Characterization of PGAamine Polymers. *^{1}H-Nuclear Magnetic Resonance (NMR).* PGA precursor was dissolved in deuterium oxide D_2O (ARMAR chemicals, Dottingen, Swizerland) supplemented with Sodium deuteroxide NaOD (Sigma-aldrich) and PGAamine was dissolved in D2O, followed by NMR spectroscopy using 400 MHz Avacne, Bruker (Karlshruhe, Germany) system.

Multi Angle Static Light Scattering (MALS). Molecular weight and polydispersity analysis of PGA polymers were performed on Agilent 1200 series HPLC system (Agilent Technologies Santa Clara, CA, US) equipped with a multi angle light scattering detector (Wyatt Technology Corporation Santa Barbara, US), using Shodex Kw404-4F column (Showa Denko America, Inc.) in PBS, flow 0.3 mL/min.

Physicochemical Characterization of Polyplexes. *Electrophoretic Mobility Shift Assay (EMSA).* Evaluation of polymer:siRNA complexation at N/P ratios between 1 to 15 was performed as follows: Samples were prepared according to the section entitled Preparation of Polyplexes. DNA loading buffer was added to the samples, and the solution was loaded on a 2% agarose gel supplemented with ethidium bromide. A voltage of 100 V was applied for 30 min. Sample's run was evaluated under UV light.

Zeta Potential Determination. The zeta-potential measurements were performed using a ZetaSizer Nano ZS instrument with an integrated 4 mW He–Ne laser (λ = 633 nm; Malvern Instruments Ltd., Malvern, Worcestershire, UK). All measurements were performed at 25 °C using folded capillary cell (DTS 1070).

Dynamic Light Scattering (DLS). DLS analysis was performed using Vasco DLS (Nano Instruments Ltd. Cordouan Technologies, Pessac, France), equipped with a 657 nm laser. Data analysis was performed according to cumulants analysis. All measurements were performed at 25 °C.

Scanning Electron Microscope (SEM). Filtered samples were dropped on a silicon wafer and blotted with cellulose paper. SEM images were taken using Quanta 200 FEG Environmental SEM (FEI, Oregon, USA) at high vacuum and 5.0 kV. Diameters were measured by measureIT software, Particle's distribution was fitted to single-pick Gaussian using OriginPro software.

Heparin Displacement Assay. The relative strength of complexation of PGAamine:siRNA polyplexes was evaluated by measuring the release of siRNA in the presence of heparin. PGAamine:siRNA polyplexes were prepared as detailed in the section entitled Preparation

DOI: 10.1021/acs.biomac.6b00555
Biomacromolecules 2016, 17, 2787–2800

of polyplexes. Polyplex solutions were incubated in the presence of 0.01−0.25 IU of heparin/50 pmol siRNA for 15 min. DNA loading buffer was added to the samples, and the samples were loaded on a 2% agarose gel supplemented with ethidium bromide. A voltage of 100 V was applied for 15 min. Sample's run was evaluated under UV light.

***In Vitro* Evaluation of Polyplexes.** *Cell culture.* Human cervical carcinoma (HeLa) and human ovarian carcinoma (SKOV-3) cells were obtained from the American Tissue Culture Collection (ATCC). HeLa cells were cultured in DMEM supplemented with 10% fetal bovine serum (FBS), 100 U/mL Penicillin, 100 μg/mL Streptomycin, 12.5 U/mL nystatin, and 2 mM L-glutamine. SKOV-3 cells were cultured in RPMI supplemented with 20% FBS, 10 mM HEPES, 1% sodium pyruvate, 100 U/mL penicillin, 100 μg/mL streptomycin, 2 mM L-glutamine. Cells were grown at 37 °C; 5% CO_2.

Flow Cytometry (FACS). HeLa and SKOV-3 cells were seeded onto six-well plate at 200 000 cells/well densities. Following 24 h, cells were treated with PGAamine: Rac1 Cy5-labeled siRNA for 4 h. Cells were washed twice with PBS, and harvested with phenol red free Trypsin. Three mL of 5% FBS in PBS solution were added, and the samples were centrifuged for 7 min at 1100 rpm. Supernatant was discharged, and cells pellets were suspended in 500 μL of 5% FBS in PBS solution. Fluorescence was read at 635 nm using FACSCalibur flow cytometer (BD Biosciences, Heidelberg, Germany).

Cellular Internalization and Intracellular Trafficking. HeLa cells were treated with PGAamine: Rac1 Cy5-labeled siRNA for 30 min, 4 and 24 h. For inhibition of endolysosomal pathway ammonium chloride was diluted up to 2 mM in Tyrode's buffer supplemented with polyplexes solution at the indicated concentration and added to the wells. The cells were fixed with 4% paraformaldehyde. Then, cells were permeabilized by incubation in Triton X-100 0.2% solution in PBS for 10 min, followed by blocking in 1:100 solution normal mouse IgG1 and normal rabbit IgG (Santa Cruz, Heidelberg, Germany). Cells were stained with mouse anti-EEA1 (BD, New Jersey, U.S) and with rabbit anti-LAMP1 (Cell Signaling Technology, Massachusetts, US) primary antibodies, and then with Goat anti mouse IgG-FITC and Goat anti rabbit IgG-Rhodamine secondary antibodies (Santa Cruz, Heidelberg, Germany). Cellular uptake of the PGAamine:Cy5-Rac1 siRNA polyplexes was followed using Leica SP5 confocal imaging systems (X60 Magnification) (Leica Microsystems, Wetzlar Germany). To demonstrate fluorescent transferrin internalization inhibition, cells were treated with either 2 mM or 30 mM ammonium chloride in Tyrode's buffer for 4 h. Transferrin-Alexa488 (ThermoFisher Scientific, Waltham, USA) was then added at a 1/50 concentration for 15 min. The cells were fixed with 4% paraformaldehyde and mounted. Slides were imaged using Leica SP8 confocal imaging systems (X60 Magnification) (Leica Microsystems, Wetzlar Germany).

In Vitro Silencing Efficacy. *In vitro* silencing of Rac1 gene by Rac1 siRNA-carrier polyplex was evaluated with psiCHECK reporter assay (Promega Madison, Wisconsin, US). One copy of a consensus target sequence of Rac1 was cloned into the multiple cloning site located downstream of the Renilla luciferase translational stop codon in the 3′-UTR region. HeLa and SKOV-3 cells (1×10^6) were seeded in 10 cm dishes and were incubated in 37 °C, 5% CO_2 for 24 h. Each cell-containing plate was transfected with 4 μg Rac1 psiCHECK-2-based plasmids using 4 μL lipofectamine 2000 (Life Technologies, Grand Island, NY). Following 5 h, cells were reseeded in 96-wells plate at final concentration of 4000 cells per well and incubated overnight. Cells expressing Rac1 siRNA reporter plasmid were transfected with Rac1 siRNA or eGFP control siRNA either complexed with PGA cationic carrier (at 100, 250, or 500 nM siRNA) or with Lipofectamine 2000 (at 50 nM siRNA) as a control or left untreated. Following 72 h, medium was completely removed from cells ,and the cells were lysed for 20−30 min in room temperature in gentle rocking by the addition of 50 μL/well Luciferase lysis solution. Renilla and Firefly Luciferase activities were measured in each of the wells of the 96 wells plate, using Dual-Luciferase Assay kit (Promega, Madison, Wisconsin, US) according to manufacturer procedure. Aliquots of 10 μL of cell lysate from each sample were transferred to a 96-well white plate. Luciferase substrate (LARII, 40 μL) was added to each extract and Firefly Luciferase activity was measured by luminescence microplate Reader (Mithras LB 940 Multimode Microplate Reader, Berthold Technologies, Germany), then 40 μL of Stop&Glo Reagent was added to each of the samples and Renilla Luciferase activity was measured immediately afterward. The Renilla luciferase activity is expressed as the percentage of the normalized activity value (Renilla luciferase/Firefly luciferase) in the tested sample relative to the normalized value obtained in cells transfected with the corresponding psiCHECK-2 plasmid only (without siRNA nor polyplex).

Cells Viability Assay. HeLa and SKOV-3 cells were seeded and treated with polyplex as described above in the section entitled *in vitro silencing efficacy*. Following 72 h, the number of viable cells was assessed by 3-(4,5-dimethylthiazol-2-yl)-2,5-diphenyltetrazolinium bromide (MTT) assay. Thirty microliters of 3 mg/mL MTT solution in PBS were added to the wells and incubated for 4−6 h. The medium was then replaced by 200 μL of dimethyl sulfoxide (DMSO) to dissolve the formazan crystals formed, and incubated for 20 min at 37 °C. Absorbance of the solution was measured at 560 nm by SpectraMax M5 plate reader (Molecular Devices, California, United States). Percent of viable cells was normalized to the viability of nontreated cells (100% viability).

SKOV-3 Cells Migration Assay. Cells migration assay was performed using modified 8 μm Boyden chambers. Prior to placing human ovarian carcinoma SKOV-3 cells on transwells' membrane, the cells were transfected with PGAamine:Rac1 siRNA polyplexes for 48 h in 6-well plate (150 000 cells/well). *In vitro* preparation and transfection was according to the section entitled Preparation of Polyplexes. Then cells were washed and added without polyplexes to the upper chamber of the transwell (100 000 cells/well) in 100 μL of DMEM without FBS. Two hours later, cells were allowed to migrate to the underside of the chamber for another 20 h by addition of medium with or without FBS (20% v/v) to the lower chamber. Cells were then fixed with ice-cold methanol and stained (Hema 3 Stain System). Next the migrated and stained cells were imaged using a Nikon TE2000E inverted microscope by 6× objective, brightfield illumination (Nikon corporation instruments, Tokyo, Japan). Quantification of migrated cells from captured images was done using NIH image software ImageJ. Percent of migrated cells was normalized to migrated cells toward FBS alone (no siRNA transfection).

***In vivo* Evaluation of Polyplexes.** *Maximum Tolerated Dose.* PGAamine:Rac1 siRNA polyplexes at N/P ratio of 5 (A, F and I) or 10 (B), at siRNA concentrations of 1−10 mg/kg were injected intravenously (i.v.) to BALB/c mice, at 400 μL/mouse. Mice were monitored for signs of toxicity up to 24 h post injection.

Statistical Analysis. Data were presented as means ± standard deviation (represented graphically as error bars). Statistical significance of PGAamine:Rac1 siRNA polyplexe's silencing activity was analyzed by One-way Analysis of Variance (ANOVA). Pairwise Multiple Comparison Procedures were analyzed by Holm-Sidak method. $P < 0.05$ was considered statistically significant.

Ethics Statement. All animal procedures were performed in compliance with Tel Aviv University guidelines approved by the Institutional Animal Care and Use Committee (IACUC).

RESULTS AND DISCUSSION

Side Chain Substituent Influence the Supramolecular Properties of Polyplexes. *Synthesis and Characterization of PGAamine Polymers A−I.* PGA precursors were synthesized using NCA polymerization as was previously described[48] and analyzed by ^{1}H NMR (Supplementary Figure 1a). Their molecular weights and polydispersity indexes were further characterized by MALS (Supplementary Table 1). In order to neutralize the effect of chain length on the various factors evaluated throughout this manuscript, PGA precursors bearing similar lengths of 6300−8500 g/mol were selected for the subsequent conjugations. PGAamine polymers A-I were synthesized using CDI coupling reagent to conjugate an amine moiety on the pending carboxylic groups of the PGA precursor

DOI: 10.1021/acs.biomac.6b00555
Biomacromolecules 2016, 17, 2787−2800

Scheme 1. (a) General Synthesis Mechanism of Conjugation of an Aminating Agent to the PGA Backbone via the Pending Carboxylic Groups, Carried out by CDI Coupling Reagent and the Subsequent Acidic Boc Deprotection of the Boc-Protected Primary Terminal Amine Group; (b) Chemical Structures Formed by Conjugation of Each Aminating Agent to the PGA Backbone

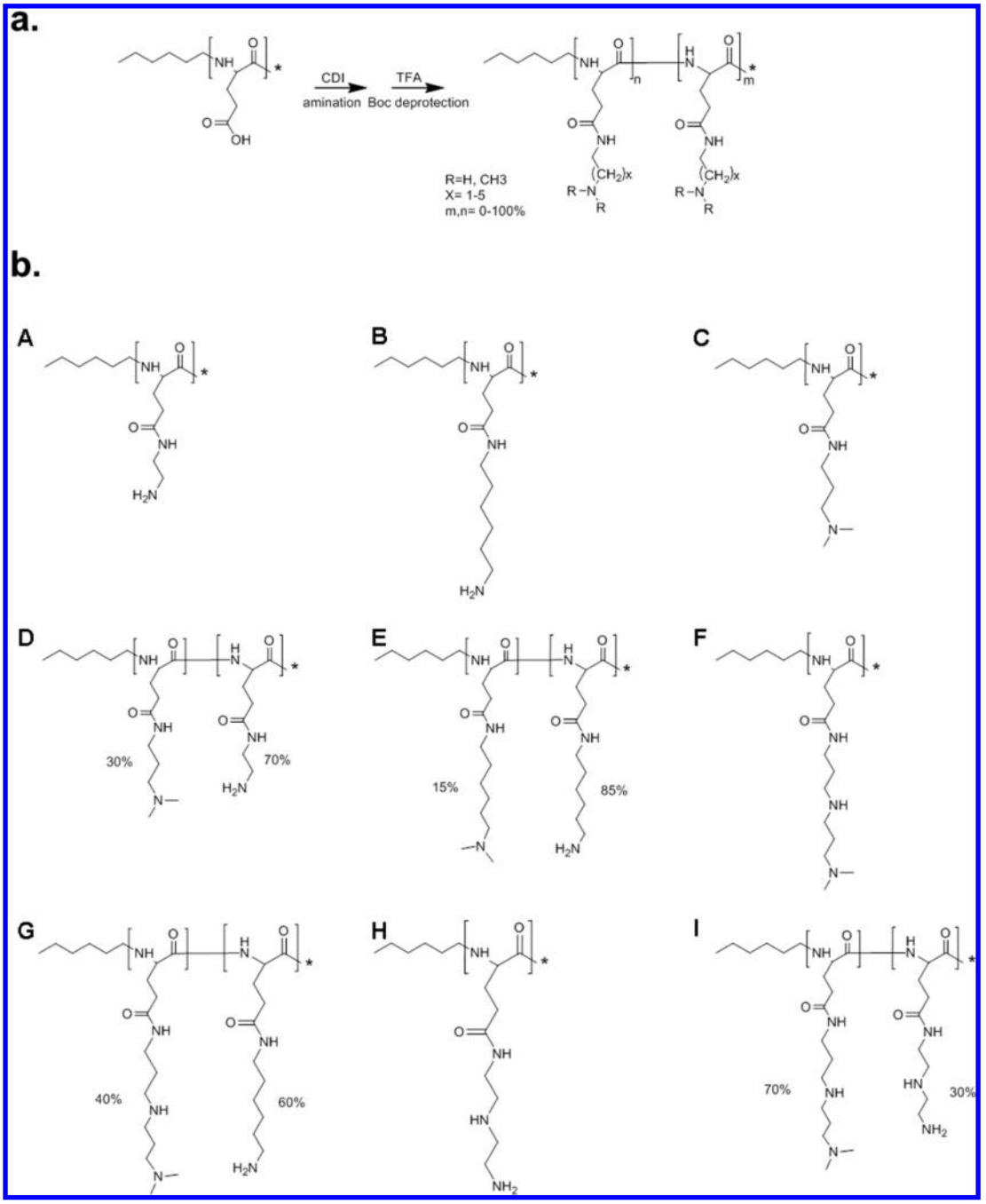

backbone (Scheme 1a). Boc protecting group was further removed by acidic deprotection. The different structures are presented in Scheme 1b.

Substitution degree was analyzed by ^{1}H NMR (Supplementary Figure 1), the peaks marked as 1, 2, and 3 represent the hydrogens of the PGA backbone, while 4 and 5 represent the hydrogens of the conjugated amine moieties. The number of corresponding hydrogens appear in brackets near the peak. For each polymer, substitution degree with each moiety was determined by dividing the integration of a representative peak of the moiety by the chiral α carbon of the PGA backbone (marked as 1, and calibrated for integration value of 1.00, corresponding to 1 hydrogen). Efficient chemical conjugation obtained by CDI reagent have allowed 100% substitution of the carboxylic groups using only 1.1 equiv of the amination reagent, while *N*,*N*′-diisopropylcarbodiimide (DIC) coupling reagent yielded 80−90% substitution degree with 5 equiv of amination reagent (polymer A, data not shown). Hybrid PGAamine polymers (D, E, G, and I) were synthesized using two different amination reagents subsequently, while final substitution ratio was controlled by the equivalents of the amination reagents, as shown by ^{1}H NMR spectra of D and E polymers

DOI: 10.1021/acs.biomac.6b00555
Biomacromolecules 2016, 17, 2787−2800

(Supplementary Figure 1). In the case ^{1}H NMR could not reveal the separate amine moieties (polymers G and I), we relied on the molar ratios of amination reagents in the synthesis to determine the substitution degree of each moiety since they gave good correlation to the analyzed substitution degree of D and E polymers, while integration of the entire hydrogens in the molecule compared to the one hydrogen adjacent to the chiral carbon helped us to conclude about the total conjugation degree of 100% (Supplementary Figure 1). The amine moieties conjugated to each polymeric backbone have varied in size and functionality: while polymer A was conjugated to "short" side chain terminated by primary amine, polymer B was conjugated to longer side chain in order to evaluate the effect of side chain's length on the size of the obtained polyplex. Polymer C was conjugated to side chain-terminated tertiary amine, in order to increase the complexation strength with siRNA and decrease the N/P ratio of their complete complexation. Successful siRNA delivery depends on fine-tuning between strong and stable complexation with the ability to release the siRNA to the cytoplasm before reaching the lysosome.[7,49] Aimed to achieve strong binding between the polymer and siRNA while maintain buffering capabilities,[46] polymers D and E were conjugated with two different moieties, each terminated by either primary or tertiary amine. The effect of side chain's length on the size of these obtained polyplexes was evaluated by using either "short" (polymer D) or longer (polymer E) side chains. Polymer F was conjugated with a side chain bearing the two amine functionalities, combining terminal tertiary amine and secondary amine on the same side chain. We further evaluated combination of the latter side chain structure with side chain terminated by primary amine (polymer G). Last two structures included functionalities of primary and secondary amine on single side chain (polymer H) or its combination with tertiary and secondary amine on single side chain at a hybrid system (polymer I). Properties such as strength of complexation between the polymer and siRNA, size and charge of polyplexes, their cellular internalization, silencing activity and toxicity were investigated in light of the various modifications introduced by structure of amine moieties.

Electrophoretic Mobility Shift Analysis of Polyplexes Composed of PGAamine Polymers A–I and siRNA. Complex formation of PGAamine A-I with siRNA was investigated by gel electrophoresis mobility shift assay (EMSA) (Figure 1a). The optimum N/P ratio for each complex was inferred from the retardation of siRNA mobility in agarose gel. Both polymers A and B have shown complete complexation starting from 2 N/P ratio. Polymer C has also complexed with siRNA at 2 N/P ratio, indicating despite our expectations, branching of the terminal amine did not affect the minimal complexation ratio. In order to evaluate the complexation strength in light of the addition of tertiary terminal amine moiety, heparin displacement assay was applied (Supplementary Figure 2). The polyanion heparin is an established indicator for the strength of complexation between cationic polymers and oligonucleotides.[50] The strength of the complexation of polyplex C (tertiary terminal amine) was higher than that of polyplex A (primary terminal amine), as indicated by the higher amount of the anion heparin required in order to displace the siRNA from its binding to the polymer (0.075 IU heparin/50 pmol siRNA compared with only 0.025 IU required in polyplex A). This stronger complexation was also approved by the decreased intensity of the ethidium bromide fluorescence at 10 N/P ratio shown in the EMSA of polyplex C. This phenomena results from exclusion of ethidium bromide from its intercalation sites

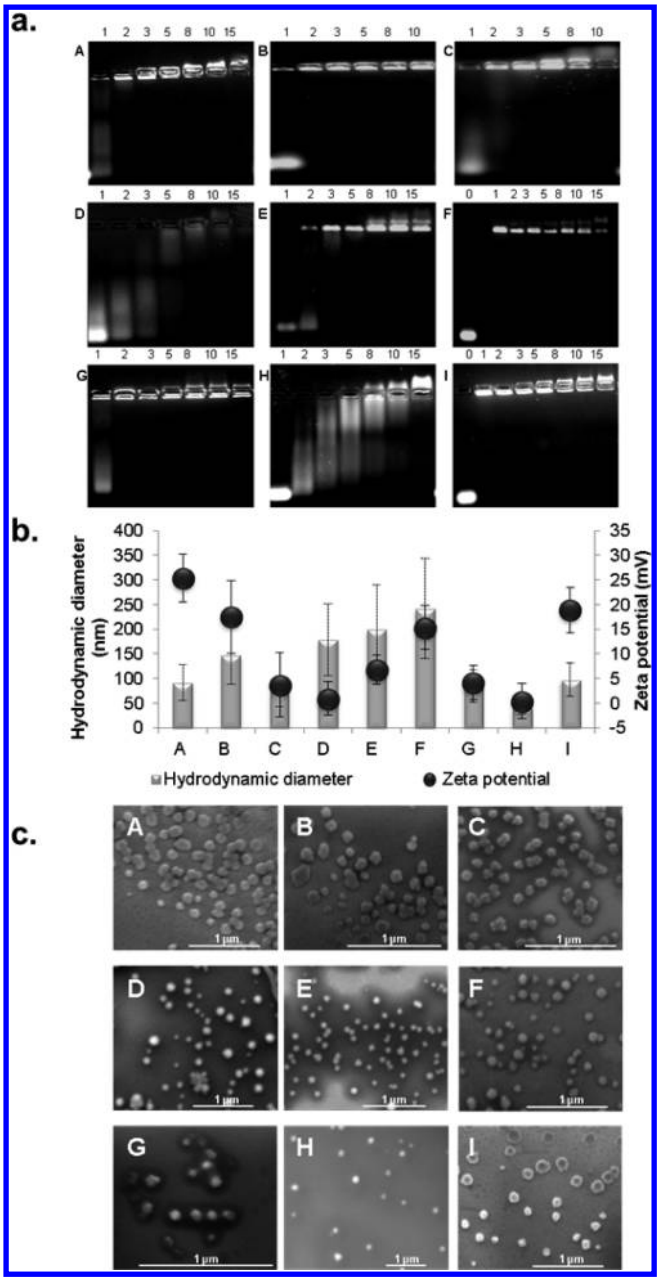

Figure 1. Physicochemical characterization of PGAamine:siRNA polyplexes. (a) Electrophoresis mobility shift analysis of polymers A–I complexed with Rac1 siRNA at nitrogen/phosphorus (N/P) ratios specified above the gel images. (b) Zeta potential and diameter values of PGAamine:siRNA polyplexes at N/P ratios of either 5 (polymers A, C, D, E, F, G, H, and I) or 10 (polymer B), as obtained by zetasizer and DLS. (c) SEM images of polyplexes A–I at the same N/P ratios used for DLS and zetasizer analyses.

with siRNA by the strong affinity of the oligonucleotides to the polymer.[51] The combination of two different side chains on one polymer—one ends with tertiary amine and the other with primary amine—seems to result in lower affinity toward siRNA and higher minimal complexation ratio, as indicated by gels D and E. Polymer E with the longer side chains had slightly better complexation qualities exhibiting 3 N/P ratio minimal complexation ratio compared to 5 N/P minimal complexation ratio obtained by polymer D. Adding a secondary amine to moieties ending by tertiary amine have restored the complexation qualities, as shown by complexation properties of polymers F and G

DOI: 10.1021/acs.biomac.6b00555
Biomacromolecules 2016, 17, 2787–2800

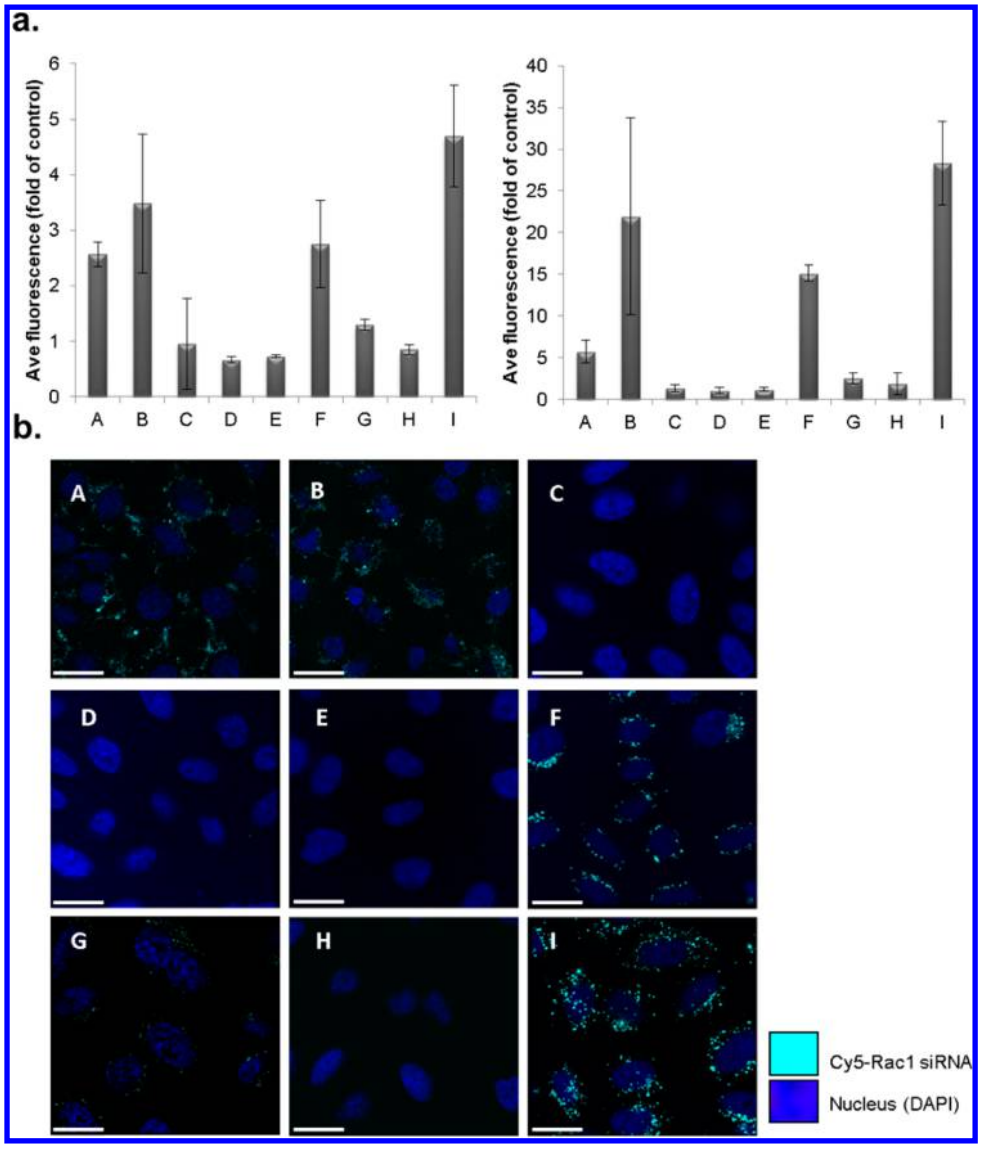

Figure 2. Cell internalization of PGAamine:Cy5-Rac1 siRNA polyplexes. HeLa and SKOV-3 cells were treated with polyplexes A–I at 100 nM concentration and N/P ratios of 5 (polymers A, C, D, E, F, G, H, and I) or 10 (polymer B) for 4 h. (a) Relative Cy5 fluorescence in HeLa (left panel) and SKOV3 (right panel) cells, indicating high intensity in cells treated with A, B, F, and I polyplexes, as obtained by FACS analysis. Bars represent average ± SD of 3 repeats. (b) Representative confocal images indicating the vast appearance of Cy5-Rac1 siRNA clusters inside HeLa cells that were treated with polyplexes A, B, F, and I. Scale bar = 20 μm.

that exhibited minimal complexation ratios of 1 and 2 N/P, respectively. The addition of a secondary amine, aimed to increase buffering capabilities, strengthened the complexation with siRNA, as demonstrated by heparin displacement assay performed on polymer F indicating that the siRNA was not displaced even in the presence of 0.25 IU heparin (Supplementary Figure 2). Adding a secondary amine to side chain that ends with primary amine (polymer H) had affected the complexation strength and charge neutralization of the polyplexes. The EMSA image shows that minimal neutralization of charge was obtained only at 10 N/P ratio. This relatively low surface charge of polyplex H at 5 N/P ratio was further approved by zeta potential analysis (Figure 1b). Complexation qualities were restored again when the latter side-chain moiety was combined with additional moiety that bears tertiary terminal amine and secondary amine, as indicated by gel I. This structure resulted in minimal complexation ratio of 1 N/P, indicating strong attraction between PGAamine polymer to siRNA.

Physicochemical Characterization of PGAamine:Rac1 siRNA Polyplexes. Zeta potential analysis of PGAamine:siRNA polyplexes was performed in order to assess surface charges of the polyplexes (Figure 1b, Supplementary Table 4). Due to method limitation the analysis was performed in 15 mM PBS and not in the polyplexe's transfection media. This may alter the physicochemical characteristics of polyplexes.[52,53] Zeta potentials of the 5 N/P ratio polyplexes A, C, D, E, F, G, H, and I and of 10 N/P ratio polyplex B have ranged between 0 to 25 mV. Polyplexes A and B, that bear side chain moieties with primary terminal amine, had relatively high zeta potentials of 25.4 ± 4.85 and 17.5 ± 7.42 mV, respectively. Interestingly, the transition to tertiary terminal amine resulted in reduced zeta potential as indicated by the charge of polyplex C (3.71 ± 6.47 mV). Combining both tertiary and primary terminal amine side chains on one backbone did not restore the high zeta potential, as indicated by charges of polyplexes D and E (0.914 ± 3.39 and 6.8 ± 2.96 mV, respectively). However, vast

DOI: 10.1021/acs.biomac.6b00555
Biomacromolecules 2016, 17, 2787–2800

addition of secondary amines to the tertiary amine-bearing moieties has resulted in increased surface charge (polyplex F with 15.3 ± 4.42 mV). Polyplex G with the low percentage of secondary amines had lower surface charge (4.13 ± 3.47 mV), while the addition of a secondary amine to a terminal primary amine backbone resulted in almost neutral zeta potential (H, 0.415 ± 3.55 mV). Polyplex I with high percentage of tertiary terminal amines and secondary amines had also high positive charge of 18.9 ± 4.62 mV. No correlation between surface charge and the length of the side chains was found. We further measured the zeta potential of higher N/P ratio polyplexes, as summarized in Supplementary Table 4. As expected, the increase in N/P ratio generally resulted in increased zeta potential. The size and morphology of 5 N/P ratio polyplexes A, C, D, E, F, G, H, and I and of 10 N/P ratio polyplex B were evaluated using DLS and SEM (Figure 1b,c, Supplementary Tables 2 and 3). DLS measurements were performed in DMEM transfection media, while SEM analysis was performed on dry sample assembled in pure water in order to avoid artifacts of dry salts and serum. Diameters have ranged between 69 to 155 nm according to SEM, and between 40 to 240 nm according to DLS, reflecting supramolecular assemblies of polymers and siRNA molecules. Particles at this size range were shown to selectively accumulate in the tumor tissue due to the enhanced permeability and retention (EPR) effect.[7,17] No correlation between size and chemical structure of the amine side chain was observed. A comparison between polyplex A (92 ± 36 nm) to B (147 ± 60 nm) and polyplex D (179 ± 73 nm) to E (201 ± 89 nm) indicated there might be slight increase in polyplexe's diameter due to increased side-chain length, although this change was not apparent by SEM resolution. Higher N/P ratio polyplexes were measured for their hydrodynamic diameter using DLS (Supplementary Table 3). Polyplexes have either increased their size or remained at nearly similar size with the increase in N/P ratio.

Supramolecular Properties of the Polyplexes, Obtained Due to Side Chain Modifications, Strongly Affect Cellular Internalization Ability and as a Result Polyplexes' Silencing Activity. *Membrane Crossing and Intracellular Trafficking of PGAamine:siRNA Polyplexes.* One of the major obstacles in the therapeutic practice of siRNA is their poor cellular penetration.[7] The ability of PGA-amine polymers to assist membrane-crossing of siRNA was quantified using Flow cytometry (Figure 2a). The protein corona adsorbed to nanoparticles in the presence of physiological fluids is a crucial factor determining their physicochemical characteristics as well as cellular uptake and trafficking mechanism, resulting in a prominent effect on intracellular silencing activity.[52,53] Therefore, PGAamine polyplexes that were initially prepared in nonsupplemented DMEM, were further added with 75% (v/v%) full medium containing either 10% FBS (for HeLa cells) or 20% FBS (for SKOV-3 cells), as detailed in the section entitled Preparation of Polyplexes. HeLa and SKOV-3 cells were transfected with the aforementioned polyplexes A–I containing Cy5-conjugated Rac1 siRNA at 5 N/P ratio (polymers A, C, D, E, F, I) or 10 N/P ratio (polymer B) for 4 h. Internalization of siRNA was evaluated at 635 nm. Relatively high Cy5 fluorescence intensity was indicated in both cell lines following treatments with polyplexes A, B, F, and I. Polyplex G demonstrated lower fluorescence intensity, while the rest of the polyplexes demonstrated low internalization capacity compared to that of Cy5-siRNA alone. Results were further validated in HeLa cells using confocal microscopy (Figure 2b). Internalization of siRNA was indicated by the appearance of punctuate Cy5-labeled structure. This pattern has appeared in cells treated with polyplexes A, B, F, and I. Lower Cy5 signal was observed in cells treated with G polyplex. During the assay, the treatment media is washed out prior to cells fixation, thus the lack of Cy5 signal indicates there was no detected cellular penetration of Cy5 conjugated siRNA. This is the case for cells treated with polyplexes C, D, E, and H. These findings fit well the flow cytometry quantification. The ability of cationic polyplexes to penetrate through cellular membranes is mostly attributed to positive surface charge.[54−56] Indeed, we have found correlation between high positive charge and better cellular internalization, as zeta potential measurements revealed higher positive charges of the internalized polyplexes (between 15 to 25 mV) while the rest of the polyplexes demonstrated lower positive-to neutral charges (between 0 to 7 mV) (Figure 1b). Yet, surface charge solely could not explain why other positively charged polyplexes such as polyplex E (6.8 ± 2.96 mV) hardly internalized to cells, while the slightly less positive polyplex G (4.13 ± 3.47 mV) showed higher internalization ability. Recent studies suggest additional mechanisms modulating cellular internalization such as hydrogen bonds with negatively charged components of cellular membranes such as carbohydrates and phospholipids, dictated by the chemical structure of the delivery vehicle and the obtained polyplex.[57] The importance of hydrogen bonds formed by cationic peptides and electron-reach domains of cellular membrane components was previously demonstrated by internalization mechanism of polyarginine.[45] Our results reveal two preferred structures of PGA conjugated- side chains in terms of cellular membrane crossing: polymers conjugated to side chains terminated by primary amine (A and B) and polymers conjugated to side chains terminated by tertiary amine that bears additional secondary amine (F and I). The importance of the secondary amine in side-chains terminated by tertiary amines is demonstrated by the inability of polymers C, D, and E, that do not bare secondary amines to internalize to cells, while polymer G with nonsufficient amount of secondary amine (only 40%) have internalized in very small amounts to HeLa and SKOV-3 cells (Figure 2a,b). Other structure such as that polymer H bears—side chain terminated by primary amine with an additional secondary amine—was unable to assist Cy5-conjugated siRNA internalization, possibly due to its almost neutral zeta potential (0.415 ± 3.55 mV).[55,56]

A large body of work was previously performed regarding the internalization mechanisms and intracellular trafficking of cationic polymers, raising both macropinocytosis, clathrin-mediated endocytosis (CME) and caveolae-mediated endocytosis (CvME) as possible parallel routes for cellular internalization of polyplexes.[58,59] Different transfection efficacies are attributed to the different pathways, raising the need in thorough examination of internalization mechanisms as a developmental tool in cationic siRNA delivery. While clathrin-coated vesicles normally fuse with acidic organelles, CvME does not necessarily include fusion with acidic organelles and hence can rescue their content from lysosomal degradation.[60] It is the CME pathway, accompanied by successful endosomal escape mechanism termed "The proton sponge effect", however, that is traditionally attributed to the successful transfection efficiency of cationic polyplexes.[46,59] This mechanism has lately gained opponents due to the discovery that poly ethylene-imine (PEI) has been accumulated in the lysosomes without causing any change in lysosomal pH.[61] The discovery of other relevant internalization pathways that do not necessarily involve fusion

DOI: 10.1021/acs.biomac.6b00555
Biomacromolecules 2016, 17, 2787−2800

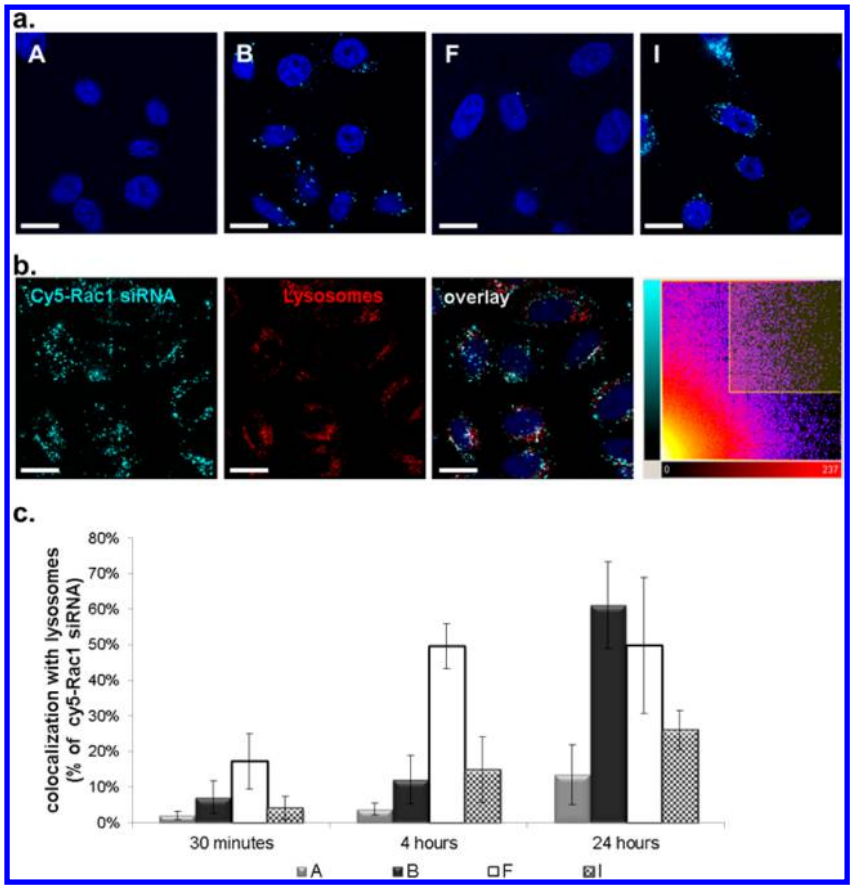

Figure 3. Intracellular trafficking of A, B, F, and I polyplexes. (a) Ammonium chloride blocked cellular internalization of A and F polyplexes. HeLa cells were treated with polyplexes A, B, F, and I at N/P ratios of 5 (polymers A, F and I) or 10 (polymer B), at 100 nM concentration and ammonium chloride at 2 mM concentration for 4 h. Scale bar = 20 μm. (B) Representative confocal images of HeLa cells treated with I polyplex for 4 h, indicating 15% colocalization with lysosomes. Scale bar = 20 μm. (c) Quantification of colocalization extent of the indicated polyplexes with lysosomes indicating time dependent accumulation in lysosomes. Bars represent the average ± SD of 6 fields.

with acidic compartments may explain discrepancies.[49] These contradicting theories raise questions regarding the preferred internalization mechanism for gene silencing. Previous studies comparing the contribution of either CME or CvME pathways to the internalization of polyethylenimine (PEI) polyplexes to HeLa cells revealed that only the CvME, and not the CME pathway, led to a successful gene transfection, although both pathways contributed to cellular internalization of polyplexes.[49,60] To address these questions, A, B, F, and I polyplexes were further tested for their internalization route and intracellular trafficking (Figure 3). Cytosolic acidification agents are well-known inhibitors of the CME pathway.[59,62] In previous studies, pH reduction was found to inhibit detachment of the formed coated-pits vesicles from the plasma membrane. Ammonium chloride treatment was demonstrated to acidify plasma of cultured cells in a mechanism attributed to the intracellular accumulation of ammonium ions.[63] Hence, the cytosolic acidification agent, ammonium chloride, was used to distinguish CME from other internalization pathways.[9,49,59] Supplementary Figure 4 demonstrates the inhibitory effect of ammonium chloride on the internalization of fluorescent transferrin, a ligand of the transferrin receptor, representing an established CME process.[64] Figure 3 shows that the internalization of polyplexes A and F was inhibited due to ammonium chloride exposure, thus their internalization is attributed mostly to the CME pathway. In agreement with previous studies,[49,60] the polyplexes internalized mostly by CME had lower silencing activity in HeLa cells than those internalized by the other pathways (Figure 4a). In SKOV-3 cells, however, all 4 polyplexes presented similar silencing efficiencies, implying intracellular trafficking is a cell-dependent mechanism.[49,60] Co-localization with late lysosomes was further evaluated using LAMP-1 lysosome-specific marker.[59] Figure 3b indicates all four polyplexes A, B, F, and I showed time-dependent increase in colocalization with lysosomes, suggesting some portion of all four polyplexes have reached the lysosomes and accumulated there. Although all 3 possible pathways (macropinocytosis, CME and CvME) might fuse with the lysosome,[59] the high extent of internalization blockage of polyplexes A and F, induced by ammonium chloride exposure (Figure 3a), in light of their gene silencing activity (Figure 4a), implies these polyplexes, that internalize by CME, used their endosomal escape capabilities in order to escape lysosomal degradation fate. Regardless of the escape mechanism, the cytoplasm is the site of activity for siRNA. The efficient gene knockdown activity of all four polyplexes indicates that at least some portion of the siRNA not colocalized with lysosomes is located in the cytoplasm, while other portions may be located at any previous stages of the endolysosomal or caveolae trafficking pathways.

Silencing Activity of PGAamine:Rac1 siRNA Polyplexes. To further evaluate the silencing potential of our PGAamine polymers as delivery vehicles of siRNA, dual luciferase reporter assay was implied (Figure 4a). HeLa and SKOV-3 cells were

DOI: 10.1021/acs.biomac.6b00555
Biomacromolecules 2016, 17, 2787−2800

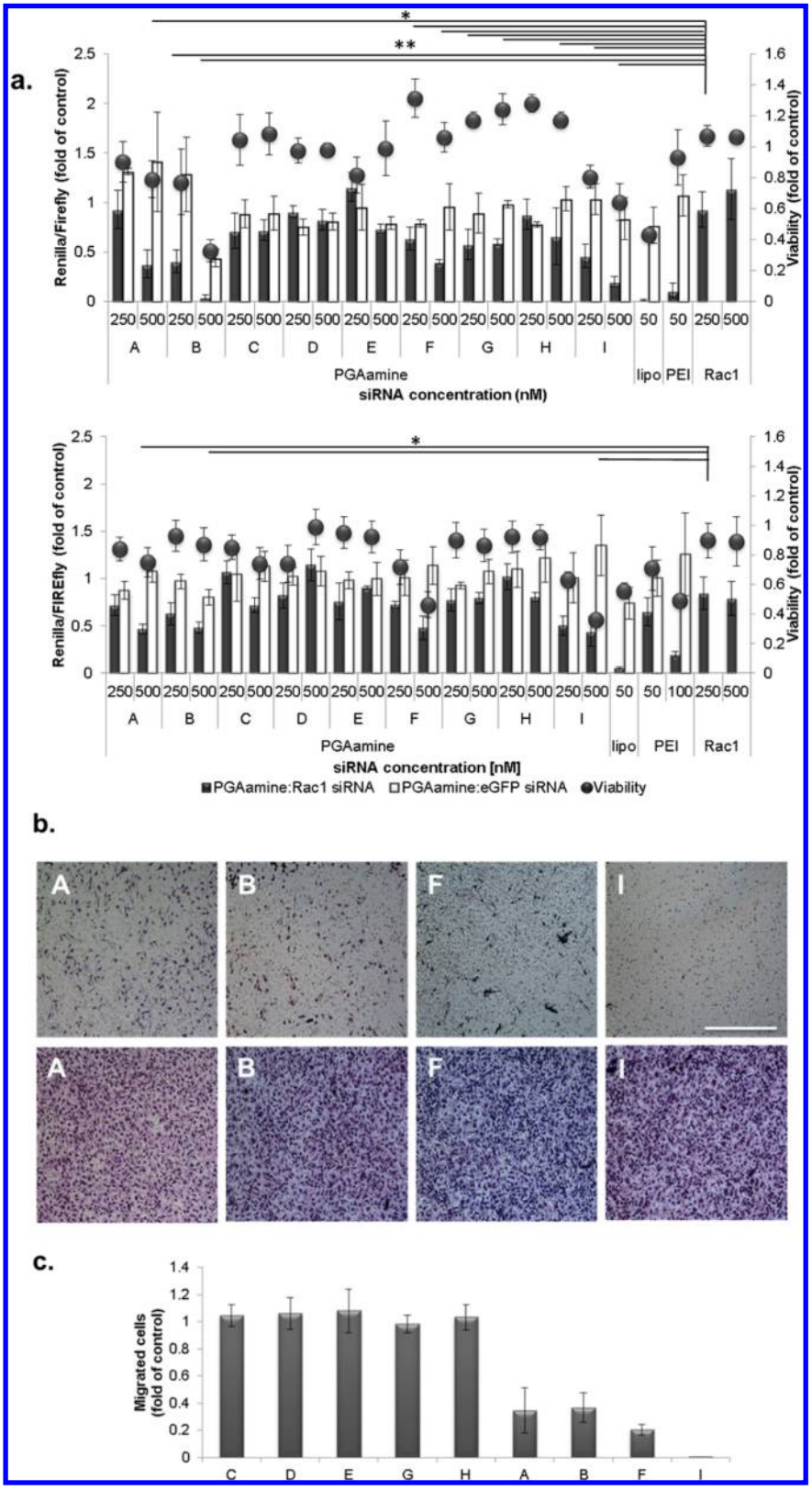

Figure 4. Activity of PGAamine:Rac1 siRNA polyplexes. (a) Silencing activity and *in vitro* toxicity values of polyplexes A–I at N/P ratios of 5 (polymers A, C, D, E, F, G, H, and I) or 10 (polymer B), as indicated by dual luciferase reporter assay (bars) and MTT assay (circles) respectively, performed on HeLa (upper panel) and SKOV-3 (lower panel) culture cells. Results are representative of 3 repeats. Bars represent the average ± SD of 4 wells. Statistical significance of silencing activities: $^{**}p < 0.001$, $^{*}p < 0.05$. (b) Transwell migration of SKOV-3 cells toward 20% FBS-containing RPMI medium following treatment with PGAamine:Rac1 siRNA (upper panel) and PGAamine:eGFP siRNA polyplexes (lower panel) A, B, F and I at 500 nM concentration and N/P ratios of 5 (polymers A, F, and I) or 10 (polymer B). Scale bar = 20 μm. (c) Quantification of the migrated cells following treatment with PGAamine:Rac1 siRNA polyplexes A–I at 500 nM concentration.

DOI: 10.1021/acs.biomac.6b00555
Biomacromolecules 2016, 17, 2787–2800

treated with polyplexes A–I for 72 h and evaluated for Rac1-mRNA knockdown. No silencing activity (lower than 0.5-fold) was exhibited by polyplexes C, D, E, G, and H at 5 N/P ratio in both cell lines. Moderate silencing activity (more than 0.5-fold silencing) was found with polyplexes A and F in HeLa cells and with polyplexes A, B, F, and I in SKOV-3 cells, while high silencing activity was obtained by polyplexes B and I (0.60- and 0.54-fold silencing at 250 nM concentration, 0.96- and 0.81-fold silencing at 500 nM concentration, respectively) in HeLa cells. Altogether, silencing pattern in both cell lines was similar, indicating the active polyplexes to be A, B, F, and I, apart from the general higher silencing activity obtained in HeLa cells. These results correlate with the internalization ability of the polyplexes. Our findings certainly show that the limiting step to successful silencing using our library of polyplexes was the ability to penetrate into cells. To better evaluate the performance of our polyplexes, we have used linear PEI and lipofectamine as positive control nanocarriers for transfection. PEI was first described as a promising polymeric vector based on efficient *in vitro* and *in vivo* gene delivery,[46] but later findings revealed high toxicity possessing an obstacle for further *in vivo* applications.[65] Same occurred with lipofectamine being an efficient lipid-based *in vitro* transfection reagent. HeLa and SKOV-3 cells were treated with 50 nM of the commercial transfection reagents jetPRIME and lipofectamine (marked PEI and lipo respectively in Figure 4) for 72 h according to the manufacturer's protocol. As shown in Figure 4a, lipofectamine was efficient but cytotoxic (<60% cell viability), while HeLa cells responded well to the PEI nanocarrier by silencing to almost 0.1 fold of the original luciferase expression level. SKOV-3 cells, however, were less sensitive to treatment with 50 nM siRNA carried by PEI. Higher concentration (100 nM) was required in order to obtain effective silencing, but was accompanied by increased cytotoxicity. Cell viability studies showed that the toxicity of our PGAamine polyplexes was strongly related to the cellular internalization ability and to a positive surface charge, with some variability within the active polyplexes between the two cell lines: while polyplex B displayed the highest activity in HeLa cells, it was also the most toxic in this cell line (retained only 0.33-fold viability at 500 nM); however, this toxicity was not apparent in SKOV-3 cell line. Polyplex F that was not toxic in HeLa cells demonstrated high toxicity in SKOV-3 cell line, retaining only 0.46 viability at 500 nM concentration. Polyplex I was toxic in both cell lines, retaining 0.65- and 0.35-fold viability at 500 nM concentration in HeLa and SKOV-3 cells, respectively. Polyplex A was slightly toxic in SKOV-3 cells retaining 0.72-fold viability at 500 nM concentration and nontoxic in HeLa cells. The nonactive polyplexes at 5 N/P ratio were all nontoxic and retained more than 78% viability. The high toxicity of the active polyplexes can be attributed to their high positive charge (zeta potential of each was higher than 15 mV).[66] It is well established that N/P ratios affect the silencing activity of cationic polyplexes.[13,29,30] In our research, we focused on N/P ratios of either 5 or 10, since these are the most applicable ratios for our polymer based delivery system. As we modified 100% of the functional pendent groups of the PGA, each added amine unit means an additional monomer. Higher N/P ratios, therefore, result in large amounts of polymer administered only as a delivery vehicle. Clinically and economically, this is an undesired scenario. We therefore defined polymers that were active at 5 or 10 N/P ratios as the preferred polymers for silencing activity. Despite the aforementioned, the activity of our library of polyplexes at higher N/P ratios than those presented in Figure 4a had an investigational value for our understanding of their structure–activity relationships. We therefore evaluated the silencing activity of polymers that were not active at 5 or 10 N/P ratios at increasing ratios up to 100 N/P. We limited the increase to the point of indicated toxicity, i.e, viability reduction to less than 0.75-fold (Supplementary Figure 5). Less than 0.5-fold activity of these polymers in HeLa cells was obtained only by G polyplex at 15 N/P ratio, alongside high toxicity. G polymeric structure is included within our preferred structures of terminal tertiary amine with additional secondary amine at the low rate of 40%, and demonstrated low cellular internalization ability at 5 N/P. Therefore, it is not surprising that this polyplex demonstrated silencing activity at higher N/P ratios. While evaluating the activity of the polyplexes on SKOV-3 cells, we found that polyplexes C and G exhibited silencing activity at 15 N/P ratio, while E polyplex was active at the higher 25 N/P ratio. Except for polyplex G evaluated on SKOV-3 cell line, all other polyplexes that were active at the high N/P ratios (15 N/P and more) were also toxic at the relevant concentrations. Other polyplexes were not active at any of the observed N/P ratios, although possessing high toxicity, demonstrating another limitation of high dosing of cationic polymers: their potential toxicity. Polyplex H, with the lowest zeta potential was not active neither toxic even at 100 N/P ratio in both cell lines. To further evaluate the biological silencing activity of polyplexes A–I, we have performed a transwell migration assay on SKOV-3 cells using 20% FBS-containing serum as incentive for migration and Rac1 siRNA as migration inhibitor. Rac1 is a member of the Rho small GTPase proteins family, and its role in cell motility in embryonic development and tumor invasiveness is well established. Recently, its role in epithelial-mesenchymal transition (EMT) toward migration and metastasis of cancer cells was demonstrated, placing Rac1 as an attractive anticancer target.[67,68] Inhibition of migration was obtained following 48 h of treatment with A, B, F, and I polyplexes composed of PGAamine and Rac1 siRNA, while polyplexes containing eGFP control siRNA were unable to inhibit cell migration (Figure 4b). Polyplexes C, D, E, G, and H composed of PGAamine and Rac1 siRNA were unable to inhibit serum-induced migration of SKOV-3 cells (Figure 4c, Supplementary Figure 6). Inhibition of serum-induced migration of SKOV-3 cells is the result of downregulation of Rac1 mRNA induced by our PGAamine:Rac1 siRNA A, B, F, and I polyplexes. These results fit well with the results obtained from the dual luciferase assay and flow cytometry internalization analysis: polymers A, B, F and I induced siRNA cellular internalization and downregulation of gene expression.

Evaluation of *In Vivo* Toxicity of PGAamine:Rac1 siRNA Polyplexes. Maximum tolerated dose (MTD) of A, B, F, and I polyplexes was performed by evaluating the viability of BALB/c mice following single i.v. injection (Table 2).

Table 2. Maximum Tolerated Dose of Polyplexes A, B, F, and I at N/P ratios of 5 (Polymers A, F, and I) or 10 (Polymer B) for *in Vivo* Treatments Injected i.v. to BALB/c Mice at 400 μL/Mouse Dose

polymer	siRNA dose [mg/kg]	polymer dose [mg/kg]
A	8	35.2
B	6	49.1
F	6	35.6
I	1	5.7

DOI: 10.1021/acs.biomac.6b00555
Biomacromolecules 2016, 17, 2787–2800

The MTD of polyplex A was the highest: above 8 mg/kg; polyplexes F and B were tolerated at above 6 mg/kg, and polyplex I was the most toxic with MTD of 1 mg/kg.

CONCLUSIONS

PGAamine polymers prepared with various terminal amine side chains were characterized for their physicochemical properties, cellular internalization, *in vitro* activity, and toxicity. We found that cellular internalization of the polyplexes correlated with positive zeta potential, but not with polyplexe's size. Two structures of amine-side chains were preferred in terms of cellular internalization and silencing activity: either linear alkyl chain that terminates by primary amine or linear alkyl chain that terminates by tertiary amine and bears secondary amine. The silencing activity of PGAamine-siRNA polyplexes was exclusively limited by the cellular uptake capability, since all vastly internalized polyplexes demonstrated silencing activity, while the nonactive polyplexes also did not internalize into cells. Nevertheless, intracellular trafficking pathways and endosomal escape capabilities are certainly modulators of the extent of silencing activity. *In vitro* toxicity was highly affected by zeta potentials and varied between cell lines. Altogether, our results present a guiding principle for the desired qualities of cationic siRNA delivery platforms. Our active polymers have demonstrated suitable MTD along with efficient *in vitro* silencing activity paving the way for further *in vivo* evaluation.

ASSOCIATED CONTENT

Supporting Information

The Supporting Information is available free of charge on the ACS Publications website at DOI: 10.1021/acs.biomac.6b00555.

^{1}H NMR spectra of PGA and PGAamine A-I polymers. Molecular weights, PDI and the calculated number of units of the PGA precursors. Summary of the radiuses of the polyplexes images as obtained by SEM. Heparin displacement assay of polyplexes A, C, and F. Z-sectioning of A, B, F and I polyplexes at 4 h. Inhibition of cellular internalization of Alexa488-Transferrin by ammonium chloride treatment. Transwell migration of polyplexes C, D, E, G and H. (PDF)

3D movie of z-stacks of A polyplex at 4 h (AVI)

3D movie of z-stacks of B polyplex at 4 h (AVI)

3D movie of z-stacks of F polyplex at 4 h (AVI)

3D movie of z-stacks of I polyplex at 4 h (AVI)

AUTHOR INFORMATION

Corresponding Author

*Address: Department of Physiology and Pharmacology, Sackler School of Medicine, Tel Aviv University, Ramat Aviv, Tel Aviv 69978, Israel. Tel: 972-3-6407427, E-mail: ronitsf@post.tau.ac.il.

Author Contributions

‖These authors contributed equally

Notes

The authors declare no competing financial interest.

ACKNOWLEDGMENTS

The Satchi-Fainaro laboratory's research leading to these results was conducted within the framework of Rimonim Consortium and the MAGNET Program of the Office of the Chief Scientist of the Israel Ministry of Industry, Trade and Labor, and has received partial funding from the European Research Council under the European Union's Seventh Framework Programme (FP/2007-2013)/ERC Consolidator Grant Agreement No. [617445] (PolyDorm). We thank Prof. Fernando Patolsky for the use of his clean-room.

REFERENCES

(1) Fire, A.; Xu, S.; Montgomery, M. K.; Kostas, S. A.; Driver, S. E.; Mello, C. C. Potent and specific genetic interference by double-stranded RNA in Caenorhabditis elegans. *Nature* **1998**, *391*, 806−11.

(2) Lee, R. C.; Feinbaum, R. L.; Ambros, V. The C. elegans heterochronic gene lin-4 encodes small RNAs with antisense complementarity to lin-14. *Cell* **1993**, *75*, 843−54.

(3) Carthew, R. W.; Sontheimer, E. J. Origins and Mechanisms of miRNAs and siRNAs. *Cell* **2009**, *136*, 642−55.

(4) Calin, G. A.; Dumitru, C. D.; Shimizu, M.; Bichi, R.; Zupo, S.; Noch, E.; Aldler, H.; Rattan, S.; Keating, M.; Rai, K.; Rassenti, L.; Kipps, T.; Negrini, M.; Bullrich, F.; Croce, C. M. Frequent deletions and down-regulation of micro- RNA genes miR15 and miR16 at 13q14 in chronic lymphocytic leukemia. *Proc. Natl. Acad. Sci. U. S. A.* **2002**, *99*, 15524−9.

(5) Kim, D. H.; Rossi, J. J. Strategies for silencing human disease using RNA interference. *Nat. Rev. Genet.* **2007**, *8*, 173−84.

(6) Dykxhoorn, D. M.; Palliser, D.; Lieberman, J. The silent treatment: siRNAs as small molecule drugs. *Gene Ther.* **2006**, *13*, 541−52.

(7) Scomparin, A.; Polyak, D.; Krivitsky, A.; Satchi-Fainaro, R. Achieving successful delivery of oligonucleotides - From physico-chemical characterization to in vivo evaluation. *Biotechnol. Adv.* **2015**, *33*, 1294−309.

(8) Lehto, T.; Wagner, E. Sequence-defined polymers for the delivery of oligonucleotides. *Nanomedicine (London, U. K.)* **2014**, *9*, 2843−59.

(9) Ofek, P.; Fischer, W.; Calderon, M.; Haag, R.; Satchi-Fainaro, R. In vivo delivery of small interfering RNA to tumors and their vasculature by novel dendritic nanocarriers. *FASEB J.* **2010**, *24*, 3122−34.

(10) Wu, Y.; Crawford, M.; Yu, B.; Mao, Y.; Nana-Sinkam, S. P.; Lee, L. J. MicroRNA delivery by cationic lipoplexes for lung cancer therapy. *Mol. Pharmaceutics* **2011**, *8*, 1381−9.

(11) McCaskill, J.; Singhania, R.; Burgess, M.; Allavena, R.; Wu, S.; Blumenthal, A.; McMillan, N. A. Efficient Biodistribution and Gene Silencing in the Lung epithelium via Intravenous Liposomal Delivery of siRNA. *Mol. Ther.–Nucleic Acids* **2013**, *2*, e96.

(12) Fehring, V.; Schaeper, U.; Ahrens, K.; Santel, A.; Keil, O.; Eisermann, M.; Giese, K.; Kaufmann, J. Delivery of therapeutic siRNA to the lung endothelium via novel Lipoplex formulation DACC. *Mol. Ther.* **2014**, *22*, 811−20.

(13) Yu, T.; Liu, X.; Bolcato-Bellemin, A. L.; Wang, Y.; Liu, C.; Erbacher, P.; Qu, F.; Rocchi, P.; Behr, J. P.; Peng, L. An amphiphilic dendrimer for effective delivery of small interfering RNA and gene silencing in vitro and in vivo. *Angew. Chem., Int. Ed.* **2012**, *51*, 8478−84.

(14) Nuhn, L.; Tomcin, S.; Miyata, K.; Mailander, V.; Landfester, K.; Kataoka, K.; Zentel, R. Size-dependent knockdown potential of siRNA-loaded cationic nanohydrogel particles. *Biomacromolecules* **2014**, *15*, 4111−21.

(15) Tiram, G.; Scomparin, A.; Ofek, P.; Satchi-Fainaro, R. Interfering cancer with polymeric siRNA nanomedicines. *J. Biomed. Nanotechnol.* **2014**, *10*, 50−66.

(16) Shi, J.; Xiao, Z.; Votruba, A. R.; Vilos, C.; Farokhzad, O. C. Differentially charged hollow core/shell lipid-polymer-lipid hybrid nanoparticles for small interfering RNA delivery. *Angew. Chem., Int. Ed.* **2011**, *50*, 7027−31.

(17) Maeda, H.; Wu, J.; Sawa, T.; Matsumura, Y.; Hori, K. Tumor vascular permeability and the EPR effect in macromolecular therapeutics: a review. *J. Controlled Release* **2000**, *65*, 271−84.

(18) Satchi-Fainaro, R.; Duncan, R.; Barnes, C. M. Polymer Therapeutics for Cancer: Current Status and Future Challenges. In

DOI: 10.1021/acs.biomac.6b00555
Biomacromolecules 2016, 17, 2787−2800

Polymer Therapeutics II: Polymers as Drugs, Conjugates and Gene Delivery Systems; Satchi-Fainaro, R., Duncan, R., Eds.; Springer: Berlin Heidelberg, 2006; Vol. *193*, pp 1−65.
(19) Millili, P. G.; Selekman, J. A.; Blocker, K. M.; Johnson, D. A.; Naik, U. P.; Sullivan, M. O. Structural and functional consequences of poly(ethylene glycol) inclusion on DNA condensation for gene delivery. *Microsc. Res. Tech.* **2010**, *73*, 866−77.
(20) Pozharski, E. V.; MacDonald, R. C. Single lipoplex study of cationic lipoid-DNA, self-assembled complexes. *Mol. Pharmaceutics* **2007**, *4*, 962−74.
(21) Bertin, A., Polyelectrolyte Complexes of DNA and Polycations as Gene Delivery Vectors. In *Polyelectrolyte Complexes in the Dispersed and Solid State II*; Müller, M., Ed. Springer: Berlin Heidelberg, 2014; Vol. *256*, pp 103−195.
(22) Zuckerman, J. E.; Gritli, I.; Tolcher, A.; Heidel, J. D.; Lim, D.; Morgan, R.; Chmielowski, B.; Ribas, A.; Davis, M. E.; Yen, Y. Correlating animal and human phase Ia/Ib clinical data with CALAA-01, a targeted, polymer-based nanoparticle containing siRNA. *Proc. Natl. Acad. Sci. U. S. A.* **2014**, *111*, 11449−54.
(23) Santel, A.; Aleku, M.; Keil, O.; Endruschat, J.; Esche, V.; Fisch, G.; Dames, S.; Löffler, K.; Fechtner, M.; Arnold, W.; Giese, K.; Klippel, A.; Kaufmann, J. A novel siRNA-lipoplex technology for RNA interference in the mouse vascular endothelium. *Gene Ther.* **2006**, *13*, 1222−1234.
(24) Iversen, F.; Yang, C.; Dagnaes-Hansen, F.; Schaffert, D. H.; Kjems, J.; Gao, S. Optimized siRNA-PEG conjugates for extended blood circulation and reduced urine excretion in mice. *Theranostics* **2013**, *3*, 201−9.
(25) Whitehead, K. A.; Langer, R.; Anderson, D. G. Knocking down barriers: advances in siRNA delivery. *Nat. Rev. Drug Discovery* **2009**, *8*, 129−38.
(26) Wang, J.; Lu, Z.; Wientjes, M. G.; Au, J. L. Delivery of siRNA therapeutics: barriers and carriers. *AAPS J.* **2010**, *12*, 492−503.
(27) Wittrup, A.; Lieberman, J. Knocking down disease: a progress report on siRNA therapeutics. *Nat. Rev. Genet.* **2015**, *16*, 543−52.
(28) Lorenzer, C.; Dirin, M.; Winkler, A. M.; Baumann, V.; Winkler, J. Going beyond the liver: progress and challenges of targeted delivery of siRNA therapeutics. *J. Controlled Release* **2015**, *203*, 1−15.
(29) Wu, Y.; Wang, W.; Chen, Y.; Huang, K.; Shuai, X.; Chen, Q.; Li, X.; Lian, G. The investigation of polymer-siRNA nanoparticle for gene therapy of gastric cancer in vitro. *Int. J. Nanomed.* **2010**, *5*, 129−36.
(30) Zhao, Q. Q.; Chen, J. L.; Lv, T. F.; He, C. X.; Tang, G. P.; Liang, W. Q.; Tabata, Y.; Gao, J. Q. N/P ratio significantly influences the transfection efficiency and cytotoxicity of a polyethylenimine/chitosan/DNA complex. *Biol. Pharm. Bull.* **2009**, *32*, 706−10.
(31) Nelson, C. E.; Kintzing, J. R.; Hanna, A.; Shannon, J. M.; Gupta, M. K.; Duvall, C. L. Balancing cationic and hydrophobic content of PEGylated siRNA polyplexes enhances endosome escape, stability, blood circulation time, and bioactivity in vivo. *ACS Nano* **2013**, *7*, 8870−80.
(32) Eldar-Boock, A.; Miller, K.; Sanchis, J.; Lupu, R.; Vicent, M. J.; Satchi-Fainaro, R. Integrin-assisted drug delivery of nano-scaled polymer therapeutics bearing paclitaxel. *Biomaterials* **2011**, *32*, 3862−74.
(33) Melancon, M. P.; Li, C. Multifunctional synthetic poly(L-glutamic acid)-based cancer therapeutic and imaging agents. *Mol. Imaging* **2011**, *10*, 28−42.
(34) Shaffer, S. A.; Baker-Lee, C.; Kennedy, J.; Lai, M. S.; de Vries, P.; Buhler, K.; Singer, J. W. In vitro and in vivo metabolism of paclitaxel poliglumex: identification of metabolites and active proteases. *Cancer Chemother. Pharmacol.* **2007**, *59*, 537−48.
(35) Duncan, R. Polymer conjugates as anticancer nanomedicines. *Nat. Rev. Cancer* **2006**, *6*, 688−701.
(36) Duncan, R. Designing polymer conjugates as lysosomotropic nanomedicines. *Biochem. Soc. Trans.* **2007**, *35*, 56−60.
(37) Rozhin, J.; Sameni, M.; Ziegler, G.; Sloane, B. F. Pericellular pH affects distribution and secretion of cathepsin B in malignant cells. *Cancer Res.* **1994**, *54*, 6517−25.
(38) Chandran, K.; Sullivan, N. J.; Felbor, U.; Whelan, S. P.; Cunningham, J. M. Endosomal proteolysis of the Ebola virus glycoprotein is necessary for infection. *Science* **2005**, *308*, 1643−5.
(39) Schornberg, K.; Matsuyama, S.; Kabsch, K.; Delos, S.; Bouton, A.; White, J. Role of endosomal cathepsins in entry mediated by the Ebola virus glycoprotein. *J. Virol* **2006**, *80*, 4174−8.
(40) Langer, C. J.; O'Byrne, K. J.; Socinski, M. A.; Mikhailov, S. M.; Lesniewski-Kmak, K.; Smakal, M.; Ciuleanu, T. E.; Orlov, S. V.; Dediu, M.; Heigener, D.; Eisenfeld, A. J.; Sandalic, L.; Oldham, F. B.; Singer, J. W.; Ross, H. J. Phase III trial comparing paclitaxel poliglumex (CT-2103, PPX) in combination with carboplatin versus standard paclitaxel and carboplatin in the treatment of PS 2 patients with chemotherapy-naive advanced non-small cell lung cancer. *J. Thorac. Oncol.* **2008**, *3*, 623−30.
(41) O'Brien, M. E.; Socinski, M. A.; Popovich, A. Y.; Bondarenko, I. N.; Tomova, A.; Bilynskyi, B. T.; Hotko, Y. S.; Ganul, V. L.; Kostinsky, I. Y.; Eisenfeld, A. J.; Sandalic, L.; Oldham, F. B.; Bandstra, B.; Sandler, A. B.; Singer, J. W. Randomized phase III trial comparing single-agent paclitaxel Poliglumex (CT-2103, PPX) with single-agent gemcitabine or vinorelbine for the treatment of PS 2 patients with chemotherapy-naive advanced non-small cell lung cancer. *J. Thorac. Oncol.* **2008**, *3*, 728−34.
(42) Paz-Ares, L.; Ross, H.; O'Brien, M.; Riviere, A.; Gatzemeier, U.; Von Pawel, J.; Kaukel, E.; Freitag, L.; Digel, W.; Bischoff, H.; Garcia-Campelo, R.; Iannotti, N.; Reiterer, P.; Bover, I.; Prendiville, J.; Eisenfeld, A. J.; Oldham, F. B.; Bandstra, B.; Singer, J. W.; Bonomi, P. Phase III trial comparing paclitaxel poliglumex vs docetaxel in the second-line treatment of non-small-cell lung cancer. *Br. J. Cancer* **2008**, *98*, 1608−13.
(43) Dipetrillo, T.; Suntharalingam, M.; Ng, T.; Fontaine, J.; Horiba, N.; Oldenburg, N.; Perez, K.; Birnbaum, A.; Battafarano, R.; Burrows, W.; Safran, H. Neoadjuvant paclitaxel poliglumex, cisplatin, and radiation for esophageal cancer: a phase 2 trial. *Am. J. Clin. Oncol.* **2012**, *35*, 64−7.
(44) Musyanovych, A.; Dausend, J.; Dass, M.; Walther, P.; Mailander, V.; Landfester, K. Criteria impacting the cellular uptake of nanoparticles: a study emphasizing polymer type and surfactant effects. *Acta Biomater.* **2011**, *7*, 4160−8.
(45) Fuchs, S. M.; Raines, R. T. Internalization of cationic peptides: the road less (or more?) traveled. *Cell. Mol. Life Sci.* **2006**, *63*, 1819−22.
(46) Boussif, O.; Lezoualc'h, F.; Zanta, M. A.; Mergny, M. D.; Scherman, D.; Demeneix, B.; Behr, J. P. A versatile vector for gene and oligonucleotide transfer into cells in culture and in vivo: polyethylenimine. *Proc. Natl. Acad. Sci. U. S. A.* **1995**, *92*, 7297−301.
(47) Yezhelyev, M. V.; Qi, L.; O'Regan, R. M.; Nie, S.; Gao, X. Proton-sponge coated quantum dots for siRNA delivery and intracellular imaging. *J. Am. Chem. Soc.* **2008**, *130*, 9006−12.
(48) Conejos-Sanchez, I.; Duro-Castano, A.; Birke, A.; Barz, M.; Vicent, M. J. A controlled and versatile NCA polymerization method for the synthesis of polypeptides. *Polym. Chem.* **2013**, *4*, 3182−3186.
(49) Rejman, J.; Bragonzi, A.; Conese, M. Role of clathrin- and caveolae-mediated endocytosis in gene transfer mediated by lipo- and polyplexes. *Mol. Ther.* **2005**, *12*, 468−74.
(50) Han, L.; Tang, C.; Yin, C. Effect of binding affinity for siRNA on the in vivo antitumor efficacy of polyplexes. *Biomaterials* **2013**, *34*, 5317−27.
(51) Geall, A. J.; Blagbrough, I. S. Rapid and sensitive ethidium bromide fluorescence quenching assay of polyamine conjugate-DNA interactions for the analysis of lipoplex formation in gene therapy. *J. Pharm. Biomed. Anal.* **2000**, *22*, 849−59.
(52) Caracciolo, G.; Callipo, L.; De Sanctis, S. C.; Cavaliere, C.; Pozzi, D.; Lagana, A. Surface adsorption of protein corona controls the cell internalization mechanism of DC-Chol-DOPE/DNA lipoplexes in serum. *Biochim. Biophys. Acta, Biomembr.* **2010**, *1798*, 536−43.
(53) Ritz, S.; Schottler, S.; Kotman, N.; Baier, G.; Musyanovych, A.; Kuharev, J.; Landfester, K.; Schild, H.; Jahn, O.; Tenzer, S.; Mailander, V. Protein corona of nanoparticles: distinct proteins regulate the cellular uptake. *Biomacromolecules* **2015**, *16*, 1311−21.

DOI: 10.1021/acs.biomac.6b00555
Biomacromolecules 2016, 17, 2787−2800

(54) Elouahabi, A.; Ruysschaert, J. M. Formation and intracellular trafficking of lipoplexes and polyplexes. *Mol. Ther.* **2005**, *11*, 336−47.
(55) Miller, C. R.; Bondurant, B.; McLean, S. D.; McGovern, K. A.; O'Brien, D. F. Liposome-cell interactions in vitro: effect of liposome surface charge on the binding and endocytosis of conventional and sterically stabilized liposomes. *Biochemistry* **1998**, *37*, 12875−83.
(56) Gratton, S. E.; Ropp, P. A.; Pohlhaus, P. D.; Luft, J. C.; Madden, V. J.; Napier, M. E.; DeSimone, J. M. The effect of particle design on cellular internalization pathways. *Proc. Natl. Acad. Sci. U. S. A.* **2008**, *105*, 11613−8.
(57) McLendon, P. M.; Buckwalter, D. J.; Davis, E. M.; Reineke, T. M. Interaction of poly(glycoamidoamine) DNA delivery vehicles with cell-surface glycosaminoglycans leads to polyplex internalization in a manner not solely dependent on charge. *Mol. Pharmaceutics* **2010**, *7*, 1757−68.
(58) Hess, G. T.; Humphries, W. H. t.; Fay, N. C.; Payne, C. K. Cellular binding, motion, and internalization of synthetic gene delivery polymers. *Biochim. Biophys. Acta, Mol. Cell Res.* **2007**, *1773*, 1583−8.
(59) Xiang, S.; Tong, H.; Shi, Q.; Fernandes, J. C.; Jin, T.; Dai, K.; Zhang, X. Uptake mechanisms of non-viral gene delivery. *J. Controlled Release* **2012**, *158*, 371−8.
(60) von Gersdorff, K.; Sanders, N. N.; Vandenbroucke, R.; De Smedt, S. C.; Wagner, E.; Ogris, M. The internalization route resulting in successful gene expression depends on both cell line and polyethylenimine polyplex type. *Mol. Ther.* **2006**, *14*, 745−53.
(61) Benjaminsen, R. V.; Mattebjerg, M. A.; Henriksen, J. R.; Moghimi, S. M.; Andresen, T. L. The possible ″proton sponge ″ effect of polyethylenimine (PEI) does not include change in lysosomal pH. *Mol. Ther.* **2013**, *21*, 149−57.
(62) Goncalves, C.; Mennesson, E.; Fuchs, R.; Gorvel, J. P.; Midoux, P.; Pichon, C. Macropinocytosis of polyplexes and recycling of plasmid via the clathrin-dependent pathway impair the transfection efficiency of human hepatocarcinoma cells. *Mol. Ther.* **2004**, *10*, 373−85.
(63) Heuser, J. Effects of cytoplasmic acidification on clathrin lattice morphology. *J. Cell Biol.* **1989**, *108*, 401−11.
(64) Le Roy, C.; Wrana, J. L. Clathrin- and non-clathrin-mediated endocytic regulation of cell signalling. *Nat. Rev. Mol. Cell Biol.* **2005**, *6*, 112−26.
(65) Xue, H. Y.; Liu, S.; Wong, H. L. Nanotoxicity: a key obstacle to clinical translation of siRNA-based nanomedicine. *Nanomedicine (London, U. K.)* **2014**, *9*, 295−312.
(66) Rezvani Amin, Z.; Rahimizadeh, M.; Eshghi, H.; Dehshahri, A.; Ramezani, M. The effect of cationic charge density change on transfection efficiency of polyethylenimine. *Iranian journal of basic medical sciences* **2013**, *16*, 150−6.
(67) Keely, P. J.; Westwick, J. K.; Whitehead, I. P.; Der, C. J.; Parise, L. V. Cdc42 and Rac1 induce integrin-mediated cell motility and invasiveness through PI(3)K. *Nature* **1997**, *390*, 632−6.
(68) Yang, W. H.; Lan, H. Y.; Huang, C. H.; Tai, S. K.; Tzeng, C. H.; Kao, S. Y.; Wu, K. J.; Hung, M. C.; Yang, M. H. RAC1 activation mediates Twist1-induced cancer cell migration. *Nat. Cell Biol.* **2012**, *14*, 366−74.

DOI: 10.1021/acs.biomac.6b00555
Biomacromolecules 2016, 17, 2787−2800